3D Numerical simulation of turbulent heat transfer and Fe_3O_4/nanofluid annular flow in sudden enlargement

Hussein Togun [1*]

[1]Biomedical Engineering Department, University of Thi-Qar, 64001 Nassiriya, Iraq

Keywords: (Abrupt enlargement, Nanofluids, Turbulent flow, Separation flow, Thermal performance)

Abstract. In this paper, 3D Simulation of turbulent Fe_3O_4/Nanofluid annular flow and heat transfer in sudden expansion are presented. k-ε turbulence standard model and FVM are applied with Reynolds number different from 20000 to 50000, enlargement ratio (ER) varied 1.25, 1.67, and 2, , and volume concentration of Fe3O4/Nanofluid ranging from 0 to 2% at constant heat flux of 4000 W/m^2. The main significant effect on surface Nusselt number found by increases in volume concentration of Fe3O4/Nanofluid for all cases because of nanoparticles heat transport in normal fluid as produced increases in convection heat transfer. Also the results showed that suddenly increment in Nusselt number happened after the abrupt enlargement and reach to maximum value then reduction to the exit passage flow due to recirculation flow as created. Moreover the size of recirculation region enlarged with the rise in enlargement ratio and Reynolds number. Increase of volume Fe_3O_4/nanofluid enhances the Nusselt number due to nanoparticles heat transport in base fluid which raises the convection heat transfer. Increase of Reynolds number was observed with increased Nusselt number and maximum thermal performance was found with enlargement ratio of (ER=2) and 2% of volume concentration of Fe_3O_4/nanofluid. Further increases in Reynolds number and enlargement ratio found lead to reductions in static pressure.

1 Introduction

Due to annular fluid flow and heat transfer characteristics are commonly used in condensers, heat exchangers, nuclear reactors, evaporator,..etc
therefore, many experimental and numerical investigation have been achieved to improve efficiency of thermal and cooling systems. Sudden expanding or contracting in cross sectional area of flow passage is one of the important technique for enhancing thermal performance. Biswas et al. [1] conducted study on influence step height of backward-facing step on characteristics of fluid flow and get that increase in separation length non-linearly and acceptable with Armaly et al. [2] because increase in step height. Also Augmentation in heat transfer was noticed by effect of contraction ratio and maximum improvement was found at contraction ratio of 1 as described by Hakan et al.[3].
Modification in transport pipeline has significant effect on thermal performance such as expanding or contracting in passage, ribbed channel, and used fins are examined in numerous numerical and experimental researches [4-18].
In the last two decades, many researches are used nanofluids as alternative fluids due to it have been greater thermal conductivity compared to normal fluids [19-28]. Kherbeet et al. [29,30] have experimentally and numerically investigated on effect using nanofluids flow in forward facing channel where determined the highest Nusselt number was about 30.6% at 1% SiO2 nanofluid. Moreover, Togun et al. [31,32] employed K-E model for analysis heat transfer characteristic and nanofluids flow through a channel with forward facing step. The results found that increase in Nusselt number with increased of volume concentrations of nanofluids, step height, and Reynolds number. However Safaei et al. [33] applied shear stress transport K-ω model to study thermal performance by using (FMWCNT) nanofluids flow over FFS. They noticed that increases in Reynolds number and volume fractions lead to rises in heat transfer coefficient.
From the previous researches, few studies adopted effects volume fractions of nanofluids with enlargement ratio and Reynolds number in annular flow passage on enhancement heat transfer rate. Therefore, the purpose of the current research is to investigate numerically the enrichment of heat transfer in abrupt enlargement of annular flow passage and the influences of volume concentrations of nanofluids, Reynolds numbers and enlargement ratio on thermal performance.

* Corresponding author: htokan_2004@yahoo.com; hussein-tokan@utq.edu.iq

2 Mathematical Model

2.1Physical Model and boundary conditions

The physical model of current paper is presented in Fig. 1A. Create geometry and meshing process by Ansys software in three dimensional as shown in Fig. 1B. The boundary condition is represented by inner pipe is insulted and has constant diameter (di) of 25 mm and length 2500 mm) while outer pipe divided into two section the inlet pipe is insulated and has different diameters (De) of 80, 60, 50 mm and length (a) of 1500 mm) while the exit pipe is heated with a constant diameter (Dt) of 100 mm and of length (b) of 1000 mm. In this simulation, the set of parameters applied to run the summations are presented in Table 1. In addition to that assumes there is no slip conditions occur between them at thermal equilibrium. Fully developed velocity was considered with hydrodynamic steady.

.

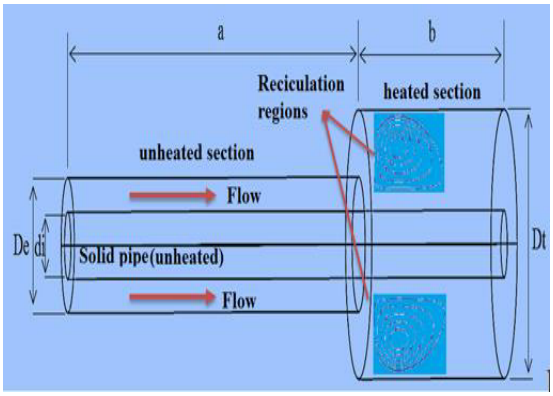

Fig. 1A. Diagram of physical model.

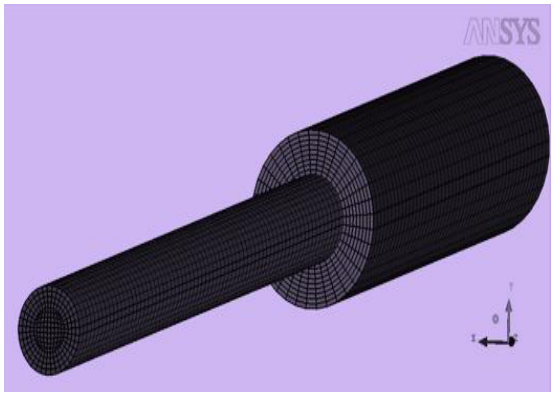

Fig. 1B. 3D Mesh.

Table 1. Boundary conditions

Reynolds number	20000, 30000, 40000, 50000
Expansion ratio (ER)	1.25, 1.67, 2
Volume fraction of Fe3O4%	0.5, 1, 1.5, 2

2.2 Physical properties of the nanofluid

In order to compute physical properties of the nanofluid specific correlations are applied. The current density of nanofluid ($\boldsymbol{\rho_{nf}}$ is calculated by eq. (1), [34]

$$\rho_{nf} = (1-\phi)\rho_f + \phi\rho_{np} \quad (1)$$

Where ρ_f and ρ_{np} are define the density of the normal fluid and the solid nanoparticles respectively.

The specific heat of the nanofluid is found by eq. (2), [34],

$$(\rho C_p)_{nf} = (1-\phi)(\rho C_p)_f + \phi(\rho C_p)_{np} \quad (2)$$

Where $(\rho C_p)_f$ and $(\rho C_p)_{np}$ are define the heat capacities of the normal fluid and the solid nanoparticles respectively.

Effective thermal conductivity of nanofluids determined by Wasp model [35] and [36]:

$$k_{eff} = k_f \left(\frac{k_p + 2k_f - 2\phi(k_f - k_p)}{k_p + 2k_f + \phi(k_f - k_p)}\right) \quad (3)$$

The effective dynamic viscosity found by eq. (4) [37]

$$\mu_{eff} = \mu_f \times (1 + 2.5 \times \phi) \quad (4)$$

2.3 Governing equations

The set equations of continuity, momentum and energy are used in three dimension form and solved based on control volume method [38]

$$\frac{\partial U_i}{\partial x_i} = 0 \quad (5)$$

$$\frac{\partial (U_i U_j)}{\partial x_j} = -\frac{\partial p}{\partial x_i} + \frac{\partial}{\partial x_j}\left(\mu \frac{\partial U_i}{\partial x_j} - \overline{\rho u_i u_j}\right) \quad (6)$$

$$\frac{\partial (U_i T_j)}{\partial x_j} = -\frac{\partial}{\partial x_i}\left(\frac{\mu}{Pr}\frac{\partial T_i}{\partial x_j} - \overline{\rho u_i t_j}\right) \quad (7)$$

To compute Reynolds stresses and heat fluxes the eqs.8 and 9 are used:

$$\overline{\rho u_i u_j} = -\mu_t \left(\frac{\partial U_i}{\partial x_j} + \frac{\partial U_j}{\partial x_i}\right) + \frac{2}{3}\delta_{ij} k \Big] \quad (8)$$

$$\overline{\rho u_i t_j} = -\frac{\mu_t}{\sigma_\theta}\frac{\partial T_i}{\partial x_j} \quad (9)$$

In the current study k-ε turbulence standard model are applied based on the turbulence kinetic energy and energy dissipation [39].

$$\frac{\partial \rho k U_i}{\partial x_j} = -\frac{\partial}{\partial x_j} + \left[\left(\mu + \frac{\mu_t}{\sigma_k}\right)\frac{\partial k}{\partial x_j}\right] + \rho(G_b - \varepsilon) \quad (10)$$

$$\frac{\partial \rho \varepsilon U_i}{\partial x_j} = -\frac{\partial}{\partial x_j} + \left[\left(\mu + \frac{\mu_t}{\sigma_k}\right)\frac{\partial \varepsilon}{\partial x_j}\right] + \rho\frac{\varepsilon}{k}(c_{1\varepsilon}G_b - c_{2\varepsilon}\varepsilon) \quad (11)$$

$$G_b = \mu_t \left(\frac{\partial u_i}{\partial x_j} + \frac{\partial u_j}{\partial x_i}\right)\frac{\partial u_i}{\partial x_j} \quad (12)$$

$$\mu_t = \rho c_\mu \frac{k^2}{\varepsilon} \quad (13)$$

All factors in k-ε model are :

$C_{1\varepsilon} = 1.44, C_{2\varepsilon} = 1.92, C_{3\varepsilon} = 0.09, \sigma_k = 1.0, \sigma_\varepsilon = 1.3,$ and $\mathrm{Pr} = 7.01$.

According to hydraulic diameter the Reynolds number are considered by equation (14)

$$Re = \frac{\rho_{nf} U D_h}{\mu_{eff}} \quad (14)$$

To achieve satisfy simulation results the standard k-ε turbulence model was certain, 2nd scheme with join between pressure and velocity is applied at SIMPLE algorithm. Every iteration and the convergence

condition in the remaining calculation was calculated and arranged where fewer than 10^{-6} for the continuity, and lesser than $10^{-7}$for the momentum and energy equations.

3 Mesh-Independent and code validation

In order to get mesh independent five sizes of mesh were considered as shown in Table 2. Fourth mesh is selected as mesh independent due to the change in average Nusselt number between the fourth and fifth mesh was less than 1%.
In this simulation the results of nanofluid flow and heat transfer over backward-facing step channel [40] were adopted for confirmation of the current model. The results from fig. 2 showed the good agreement between results of current model and results of Al-aswadi et al. [40].

Table 2. Mesh independent for pure water at ER=2 and Re=20000.

Size of mesh	X=30, Y=30, Z=300	X=2, Y=20, Z=500	X=20, Y=20, Z=750	X=30, Y=30, Z=750	X=20, Y=20, Z=1000
Grid no.	1	2	3	4	5
Nu_{ave}	1233.43	1246.7	1247.764	1248.151	1248.237

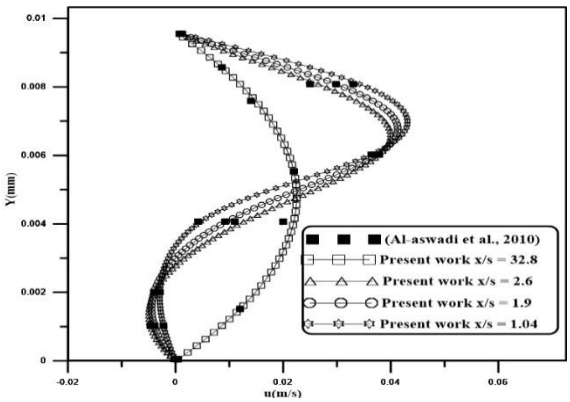

Fig. 2. Comparison velocity profile with (Al-aswadi et al., 2010)

3 Results and discussion

Figs. 3A and 3B showed that influence of enlargement ratio on Nusselt number for pure water and Fe_3O_4 nanofluid at Reynolds number of 50,000 respectively. The results revealed that sudden increases in Nusselt number occurred after the abrupt enlargement and extent to maximum value then decrease to the exit passage flow due to recirculation flow as created. It's also can be seen that the highest value of Nusselt number move far from the step heights and decreases gradually towards the exit of passage. Moreover the maximum Nusselt number found at enlargement ratio of 2 in compared with other cases.

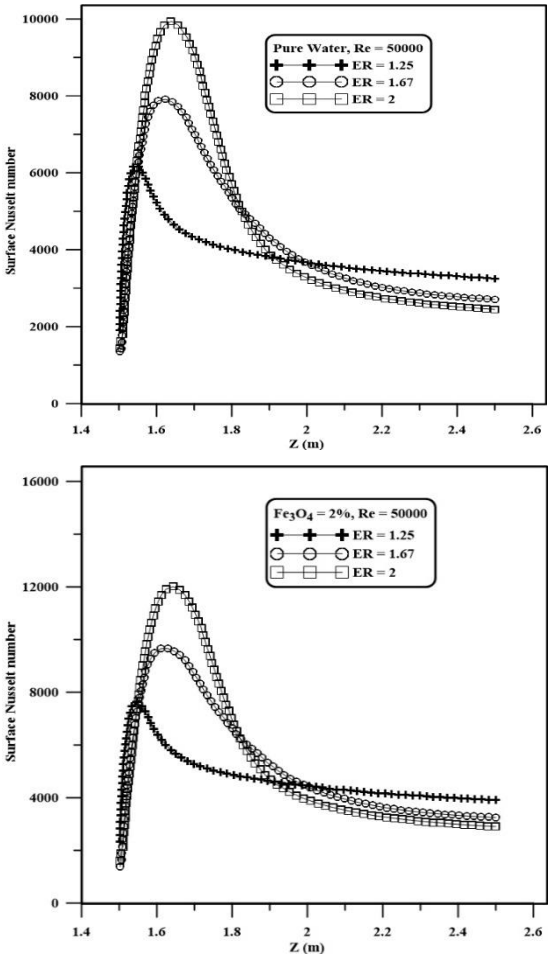

Fig. 3 Distribution of surface Nusselt number at different enlargement ratio and Re=50,000 for **A**. pure water **B**. 2% Fe3O4 nanofluid

Distributions of local Nusselt number at different Reynolds number with enlargement ratio of 2 are presented in Figs. 4A and 4B for water and 2% of Fe_3O_4 nanofluid respectively. Increases in Reynolds number observed effect on increases of local Nusselt number due to increases flow rate and the peak of profile Nusselt number noticed nearer to corner of abrupt enlargement results of separation flow as created.

Fig. 5 shows that the effect of volume concentrations of Fe_3O_4 nanofluid on local Nusselt number at enlargement ratio of 2 and Reynolds number of 50000. Increase in volume concentration Fe_3O_4/nanofluid observed lead to enhance the Nusselt number due to nanoparticles heat transport in base fluid which raises the convection heat transfer rate. The findings denoted that the highest of Nusselt number was happened at 2% volume concentration of Fe_3O_4 nanofluid and Reynolds number of 50000. For more explanation the profile of static pressure at different Reynolds number and enlargement ratios are presented in Fig 6 and 7 respectively. For all cases reduction in local static pressure at entry section of abrupt enlargement and then suddenly augmented to converge near the exit for all cases. It can be seen from the result increases in Reynolds number and enlargement ratio lead to decreases in static pressure and the local static pressure have been same trends and the lowest static pressure detected at enlargement ratio 2 and Reynolds number 50000.

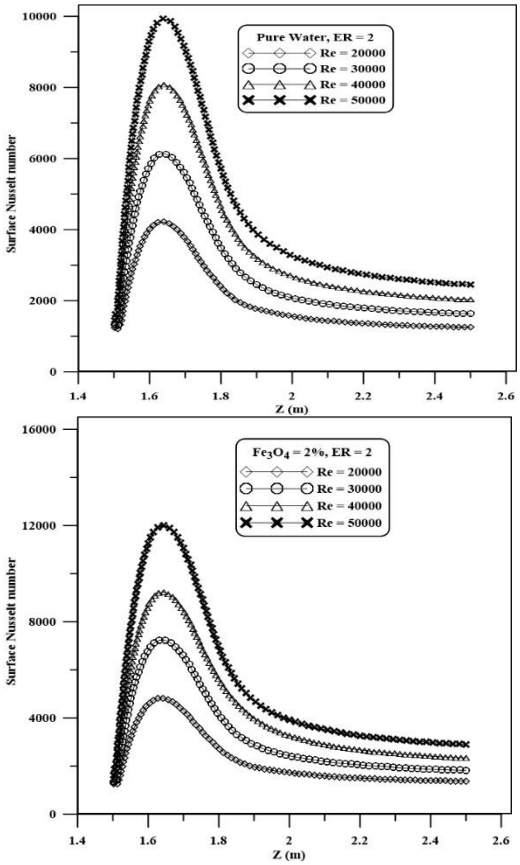

Fig. 4 Influence of Reynolds number on Nusselt number profile at ER=2 and q=4000 W/m2 for **A**. pure water **B**. 2% of Fe3O4 nanofluid

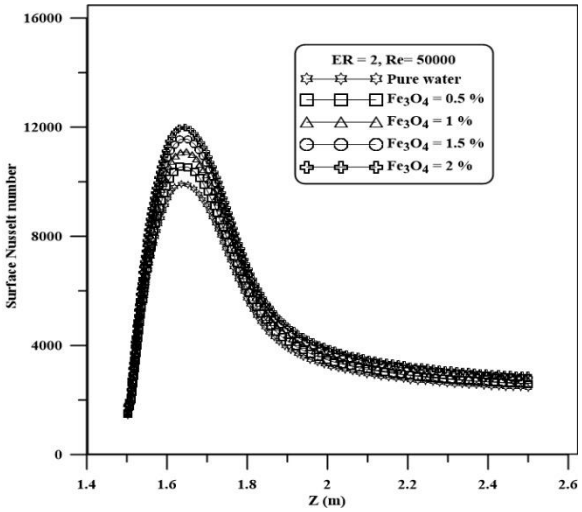

Fig. 5 Variation of surface Nusselt number at Re= 50,000 and ER= 2 for pure water and different concentrations of Fe_3O_4 nanofluid

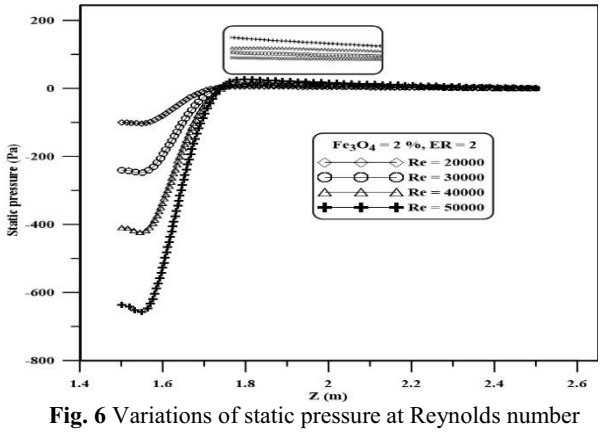

Fig. 6 Variations of static pressure at Reynolds number of 50,000 and different enlargement ratios

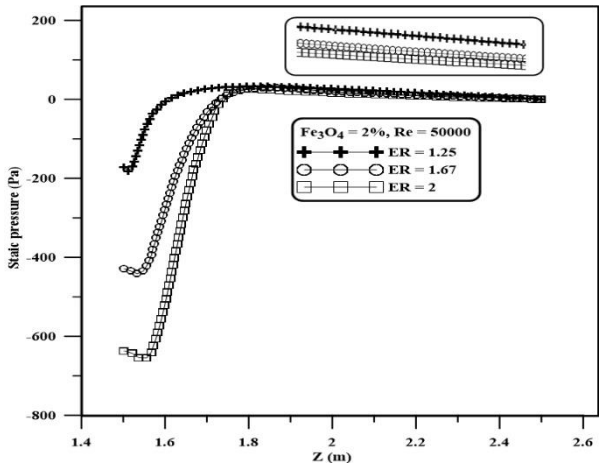

Fig. 7 Variations of static pressure at enlargement ratio of 2 and different Reynolds number

4 Conclusion

3D numerical simulation of turbulent Fe3O4/Nanofluid annular flow and heat transfer in abrupt enlargement are considered in this research. The numerical results illustrated to rapid rises in Nusselt number happened after the abrupt enlargement and extent to maximum value then reduction to the exit passage flow due to recirculation flow as produced. For all cases the peak of profile Nusselt number observed move far from the step heights and decreases gradually towards the exit of passage. Also the maximum Nusselt number found at enlargement ratio of 2 in compared with other cases and increases in Reynolds number observed effect on increases of local Nusselt number due to increases flow rate. Rise in volume concentration Fe_3O_4/nanofluid found lead to augment the Nusselt number due to nanoparticles heat transport in normal fluid which increases the convection heat transfer rate. It's also indicated that the maximum of Nusselt number was occurred at 2% volume concentration of Fe_3O_4 nanofluid

and Reynolds number of 50000. Increases in Reynolds number and enlargement ratio found lead to reductions in static pressure and the local static pressure have been same trends and the lowest static pressure noticed at enlargement ratio 2 and Reynolds number 50000.

References

1. G. Biswas, M. Breuer, F. Durst, Backward-facing step flows for various expansion ratios at low and moderate Reynolds number, Journal of Fluids Engineering, **126**: pp362-374, (2004)
2. B.F. Armaly, F. Durst, J.C.F. Pereira, B. Schonung, Experimental and theoretical investigation of backward-facing step flow, Journal of Fluid Mechanics, **127**: pp473-496, (1983)
3. H.F., Oztop. Mushatet. K.S., I. Y11maz, Analysis of turbulent flow and heat transfer over a double forward facing step with obstacles, International Communications in Heat and Mass Transfer, **39**(9) :pp1395-1403, (2012).
4. V. SriHarsha S.V. Prabhu, R.P. Vedula, Influence of rib height on the local heat transfer distribution and pressure drop in a square channel with 90° continuous and 60° V-broken ribs,Applied Thermal Engineering, **29**(11-12) :pp2444-2459, (2009).
5. H. Togun, R. Homod, T. Abdulrazzaq, HYBRID AL2O3-CU/WATER NANOFLUID FLOW AND HEAT TRANSFER OVER VERTICAL DOUBLE FORWARD-FACING STEP, Thermal science, **5A**, (2021).
6. P. Promyoog, Heat transfer and pressure drop in a channel with multiple 60° V-baffles, International Communications in Heat and Mass Transfer, **37**(7) :pp835-840, (2010).
7. H. Togun, Hakim, S. Sultan, Irfan Anjum, S.N. Kazi, An experimental study of turbulent heat transfer separation external in an annular passage, International Conference on Applications and Design in Mechanical Engineering (ICADME 2009), Universiti Malaysia Perlis (UniMAP) (2009).
8. M. SHERRY, LO JACOO:D. & SHERIDAN J, An experimental investigation of the recirculation zone formed downstream of a forward facing step. J. Wind Engng. Ind. Aerodyn **98** :pp. 888-894, (2010).
9. H. Togun, S.N. Kazi, A. Badarudin, A Review of Experimental Study of Turbulent Heat Transfer in Separated Flow, Australian Journal of Basic and Applied Sciences, **5**, pp.489- 505, (2011)
10. D. LANZERSTORFER & H.C. KUHLMANN, Three-dimensional instability of the flow over a forward-facing step, J. Fluid Mech. **695** :pp. 3904., (2012).
11. H. Togun. Y.K. Salman, H.S. Sultan Aljibori and S.N . Kazi, An experimental study of heat transfer to turbulent separation fluid flow in an annular passage, International Journal of Heat and mass Transfer, **54**(4) :pp766-773, (2011).
12. A. Gupta,V. SriHarsha, S.V. Prabhu, RP. Vedula Local heat transfer distribution in a square channel with 90° continuous, 90° saw tooth profiled and 60° broken ribs, Experimental Thermal and Fluid Science, **32**(4} :pp.997-1010, (2008).
13. C.S. Oon, H. Togun, S.N. Kazi, A. Badarudin and E. Sadeghinezhad, Computational simulation of heat transfer to separation fluid flow in an annular passage, International Communications in Heat and Mass Transfer, **46** :pp92-96, (2013).
14. D. Lanzerstorfer and H.C. Kuhlmann, Three-dimensional instability of the flow over a forward-facing step, J. Fluid Mech., 695 :pp390-404, (2012).
15. T. Hussein, S.N. Kazi, Abdul Amir H. Kadhum, A.Badarudin, MK.A. Ariffin. E. Sadeghinezhad Numerical Study of Turbulent Heat Transfer in Separated Flow :Review, International Review of Mechanical Engineering (IREME) **7**: pp337-349, (2013).
16. M. Sherry, Lo. Jacono,D. & Sheridan, J., An experiment al investigation of the recirculation zone formed downstream of a forward facing step. J. wind Engng Ind. Aerodyn. **98** :pp888-894, (2010).
17. H. Togun, T. Abdulrazzaq, S.N. Kazi, A. Badarudin and MKA. Ariffin, Heat Transfer to Laminar Flow over a Double Backward v-Facing Step" International Journal of Mechanical, Industrial Science and Engineering, **7**(2) :pp 673-678, (2013).
18. H. Hattori. and Y. Nagano, Investigation of turbulent boundary layer over forward- facing step via direct numerical simulation, Intl J Heat Fluid Flow **31**(3) :pp284-294, (2010).
19. H. Togun., T. Abdulrazzaq, S.N. Kazi, M.K.A. Arifiin, Numerical study of turbulent heat transfer in annular pipe with sudden contraction, Applied mechanics and materials **465-466** :pp461-466, (2014).
20. T. Hussein, Abu-Mulaweh, S.N. Kazi, A. Badarudin., Numerical simulation of heat transfer and separation Al2O3/nanofluid flow in concentric annular pipe: International Communications in Heat and Mass Transfer, **71** :pp108-117, (2016).
21. T. Abdulrazzaq, T. Hussein, M. Goodarzi, SN Kazi, MKA. Ariffiin, NM Adam, Kamel Hooman, Turbulent heat transfer and nanofluid flow in an annular cylinder with sudden reduction, Journal of Thermal Analysis and Calorimetry, **141** :pp373-385, (2020).
22. T. Abdulrazzaq, H. Togun, S. M. Reza, SN Kazi, MKA Ariffin, NM Adam, Effect of flow separation of TiO2 nanofluid on heat transfer in the annular space of two concentric cylinders, Thermal Science, **24** :pp1007-1018, (2020).
23. T. Hussein, Laminar CuO-water nano-fluid flow and heat transfer in a backward-facing step with and without obstacle, Applied Nanoscience, **6**(3) :pp371-378, (2016).
24. T. Abdulrazzaq, Hussein T., H. Alsulami, M. Goodarzi, M.R., Safaei, Heat Transfer Improvement in a Double Backward-Facing Expanding Channel Using Different Working Fluids, Symmetry, **12**(7) :pp1-23, (2020).
25. T. Hussein, S.N. Kazi, A Badarudin, Turbulent heat transfer to separation flow in annular concentric

pipe, International Journal of Thermal Sciences **117** :pp14-25, (2017).
26. S. Salman, Abd Rahim Abu Talib, Numerical study on the turbulent mixed convection heat transfer over 20 Microscale backward facing step, CFD Letters, **11**(10) :pp31-45, (2019).
27. H. Togun, Experimental and numerical study of heat transfer to nanofluid flow in sudden enlargement of annular concentric pipe, PhD thesis, University of Malay, (2015).
28. M. Hassan, R Sadri, G. Ahmadi, M. Dahari, S.N. Kazi, M.R., Safaei. E. Sadeghigezhad, Numerical Study of Entropy Generation in a Flowing nanofluid used in Micro- and Minichannels, Entropy, **15**(1) :pp144-155, (2013).
29. A.Sh. Kherbeet. H.A Mohammed, K.M. Munisamy, B.H. Salman, Combined convection nanofluid flow and heat transfer over microscale forward-facing step, Int. l Nanoparticle **6** (4) :pp. 350-365, (2013).
30. ASh. Kherbeet, H.A Mohammed, K.M. Munisamy, R. Saidur, B.H. Salman, I.M. Mahbubl, Experimental and numerical study of nanofluid flow and heat transfer over microscale forward-facing step, International communication in heat and mass transfer, **57** :pp319-329, (2014).
31. T. Hussein AJ. Shkarah, S.N. Kazi, A. Badarudin, CFD simulation of heat transfer and turbulent fluid flow over a double forward-facing step, Mathematical Problems in Engineering, **2013** :pp1-10, (2013).
32. H. Togun., G. Ahmadi, T. Abdulrazzaq, AJ. Shkarah, S.N. Kazi, A. Badarudin, Thermal performance of nanofluid in ducts with double forward-facing step, Journal of the Taiwan Institute of Chemical Engineers, **47** :pp28-42, (2015).
33. M.R. Safaei, T. Hussein, K Vafai, S.N. Kazi, A Badarudin, Investigation of heat transfer enhancement in a forward-facing contracting channel using FMWCNT Numerical Heat Transfer, Part A: Applications , **66** :pp1321-1340, (2014).
34. R.S. Vajih, D.K. Das, Experimental determination of thermal conductivity of three and development of new correlations, International Journal of Heat and Mass Transfer, **52**(21-22) :pp4675-4682, (2009).
35. Y. Xuan, W. RoetzeL, Conceptions for heat transfer correlation of nanofluids International Journal of Heat and mass Transfer, **43**(19) pp.3701-3707, (2000).
36. H. L. B.-X Wang, X.F. Peng, Research on the heat-conduction enhancement for liquid with particle suspensions, General Paper (G-1), International Symposium on Thermal Science and Engineering (TSE2002), Beijing, (2000).
37. H.C. Brinkman, The Viscosity of Concentrated Suspensions and Solutions, The Journal of Chemical Physics, **20**(4) :pp571-571, (1952).
38. K.G. Herrmann Schlichting, Boundary-Layer Theory, Springer, Berlin, Heidelberg, (2017).
39. Launder, B. E.; Sharma, B. I., Application of the energy-dissipation model of turbulence to the calculation of flow near a spinning disc, Letters in Heat and Mass Transfer, **1** :pp131-137, (1974).
40. A.A. Al –aswadi, H.A. Mohammed, NH. Shuaib, A. Campo, Laminar forced convection flow over a backward facing step using nanofluid International Communications in Heat and Mass Transfer, **37**(8) :PP950-957, (2010).